Practical equivalent offset processing

John C. Bancroft

ABSTRACT

The equivalent offset method of processing continues to be a practical and useful tool in the seismic industry. However, some users have reported problems with their implementations, such as being noisier in the shallower parts of the section, or the presence of some unexpected aliasing noise.

Three items for improving the results are presented; the first a parameter selection, the second is an algorithm feature, and third the possible inclusion of an antialiasing filter.

INTRODUCTION

The equivalent offset method (EOM) (Bancroft et al., 1998) of processing forms prestack migration gathers that are referred to as equivalent offset (EO) gathers. Each input trace is summed into each gather at offsets designed to represent the raypath geometry rather than the source-receiver offset. This is achieved by replacing the location of the source and receiver by a collocated source and receiver at an equivalent offset h_e that preserves the original traveltime of the trace. In effect, the double-square-root (DSR) equation that defines the traveltime t,

$$t = \sqrt{\frac{T_0^2}{4} + \frac{\left(x+h\right)^2}{V^2}} + \sqrt{\frac{T_0^2}{4} + \frac{\left(x+h\right)^2}{V^2}}\ , \tag{1}$$

is equated to a single square-root equation,

$$t = \sqrt{T_0^2 + \frac{4h_e^2}{V^2}}\ , \tag{2}$$

where x is the distance between the CMP location and the surface location of the scatterpoint, h the source-receiver half offset, T_0 the vertical zero-offset two-way time, and V the velocity. Solving for the equivalent offset, we get

$$h_e^2 = x^2 + h^2 - \frac{4x^2h^2}{T^2V^2}\ . \tag{3}$$

Reflection energy that is located at the equivalent offset will be aligned along a hyperbolic path in an EO gather. This energy is focused at the reflector position but will dissipate at all other locations. Moveout correction and stacking of the gathers complete the prestack migration.

The formation of the EO gathers requires no time-shifting of the prestack data, and is insensitive to velocities. However, after the gathers are formed, accurate velocities are then estimated for the moveout correction.

The method has application for time and depth migration, converted-wave processing, vertical seismic profiles (VSP's), vertical marine cables, borehole imaging, rugged topography, etc.

Some implementations may have a noisier shallow section when compared with other methods that use harsh antialiasing filtering. Other aliasing noise may appear on the section that may vary with the value of parameters that were selected.

The basic formation of the EO gather includes a natural antialiasing filter. This filter is a boxcar shape that that is smaller than the optimum size but appears adequate for normal processing. The inclusion of an additional antialiasing filter can reduce additional high frequency noise that may be beneficial when deconvolution is applied after migration.

Model

Prestack data was created from a simple constant velocity model that was comprised of a scatterpoint, a short horizontal event, and a dipping event with a gap. Because of its shape, it is referred to as the "hockey stick" model. The prestack data has 101 sources with 96 traces, centre-spread. Two seconds of data were recorded at 4 ms intervals with sources and receivers at 200 ft intervals. The velocity is 10,000 ft/sec, and the maximum offset approximately 10,000 ft. Reflections were located and constant amplitudes interpolated between each sample, then each trace was band-pass filtered to leave a maximum frequency of 50 Hz. No diffraction energy was computed from the edges of the reflectors, creating overshooting in the migrations. An example of one shot, at the centre of the model and an EO migration is shown in Figure 1.

The main feature of interest in this model is the scatterpoint; however, the energy of one input trace (4825) will be isolated and used to demonstrate effects on the prestack migration ellipse.

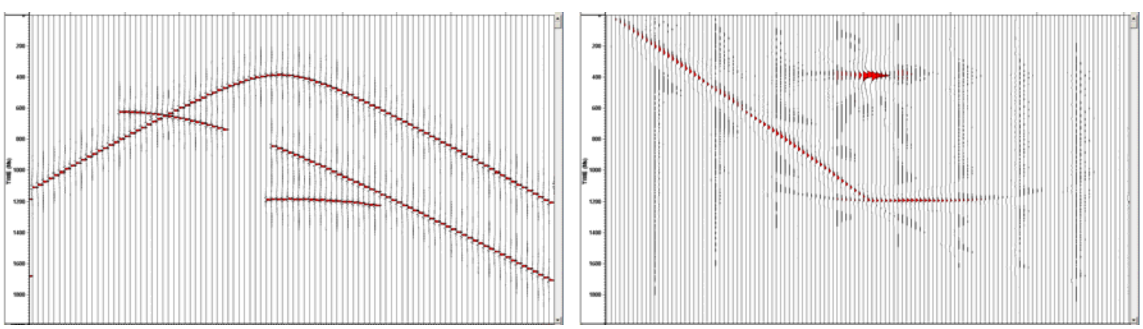

FIG. 1. a) Example of a source record near the centre of the model. b) An example of the migration.

All the prestack energy from the scatterpoint will be aligned along a hyperbola of the EO gather that is located at the scatterpoint. A few gathers away from the scatterpoint, the energy will be dispersed, as illustrated in Figure 2. This figure contains the EO gather located at the scatterpoint (a) before moveout (MO) correction, and (b) with moveout correction. Stacking this gather produces the spike of energy at the scatterpoint location. A second EO gather that is removed from the location of the scatterpoint shows this same energy that is now dispersed in (c) and after MO correction in (d). This dispersed energy stacks destructively, leaving no event.

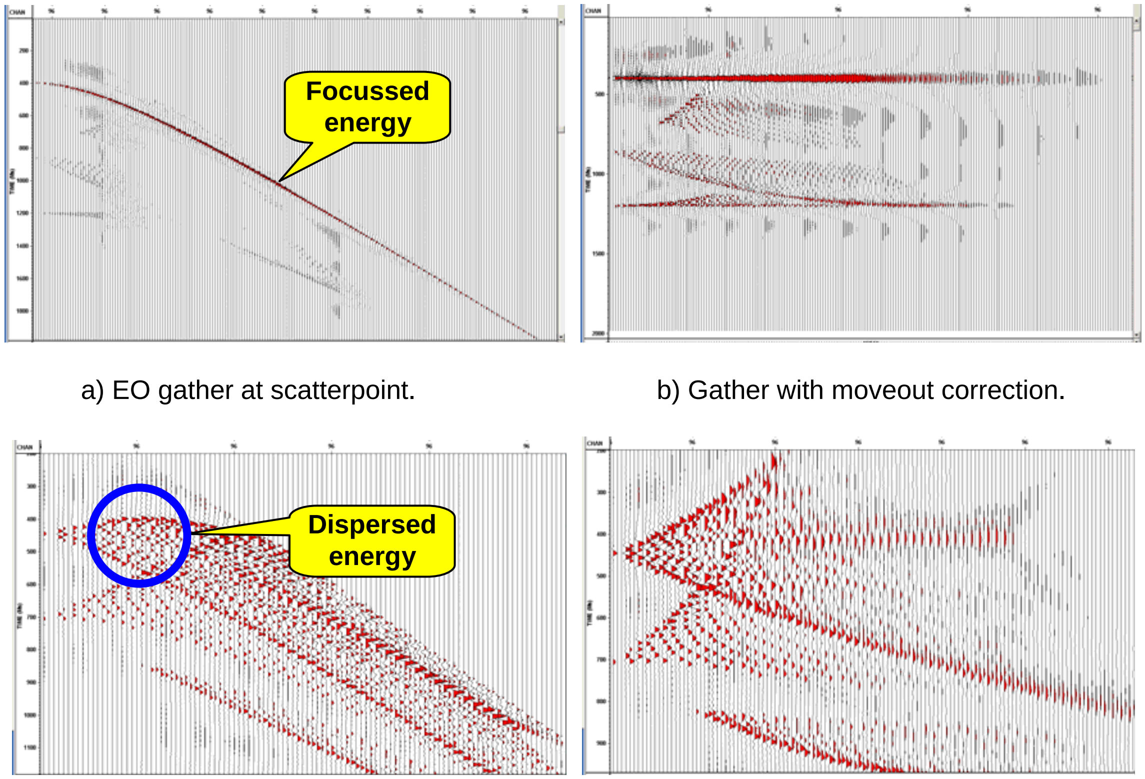

a) EO gather at scatterpoint.

b) Gather with moveout correction.

c) EO gather removed from scatterpoint.

d) Gather with moveout correction.

FIG. 2. Example of EO gathers, a) at the scatterpoint location, then b) with moveout correction, c) an EO gather removed from the scatterpoint location, and d) the moveout corrected gather.

SELECTION OF BIN SIZE

A major parameter to choose in EO processing is the bin size for the gathers. A good starting place is the same size as the CMP trace interval, which should have been chosen to eliminate aliasing of dipping energy. A second choice is to define the bin interval using the aliasing Equation (4) that relates the bin interval δh to the maximum frequency f, velocity V, and dip θ, i.e.,

$$\delta h = \frac{V}{4 f \tan\theta}. \tag{4}$$

Seismic energy, before migration, is limited to apparent dips that are less than 45 degrees. Therefore, when we substitute the model parameters into the above equation, we find the data in our model is aliased, and that the maximum frequency should be 25 Hz, or that the maximum CMP trace interval should have been 50 ft to prevent aliasing. Fortunately, we can choose any size for the bin interval and an appropriate choice is 50 ft.

There is, however, another factor that should be considered. I will only illustrate the problem with an example taken from the modelled data. The problem occurs when the bin interval equals the CMP interval. In this condition, scattered energy in a gather that is well removed from the scatterpoint may not completely cancel when stacked. However, choosing a bin interval half that size allows the moveout correction to place the energy so that it will cancel. This concept is illustrated in Figure 3, which shows moveout corrected EO gathers with a bin interval in (a) equal to the CMP interval of 100 ft, and (b) half the CMP interval or 50 ft. This effect is independent of the input data being aliased. Note the formation of coherent energy that is encircled in (a) that will create noise energy when stacked. This same energy in (b) has alternating amplitudes that tend to cancel more effectively when stacked. Corresponding stacks in (c) and (d) show the effects of the bin size on the migrated results.

Note that, in order to see this effect, the fold in the encircled area is very high, and no scaling has been applied to compensate for this high amplitude relative to those of the shorter offsets (i.e., a fold division). In addition, these displays have long offsets and large amplitude scaling to make these effects visible. The amplitude of the coherent noise is well below the amplitude of the energy at the scatterpoint. It is only shown to emphasize a potential problem that can be corrected if required.

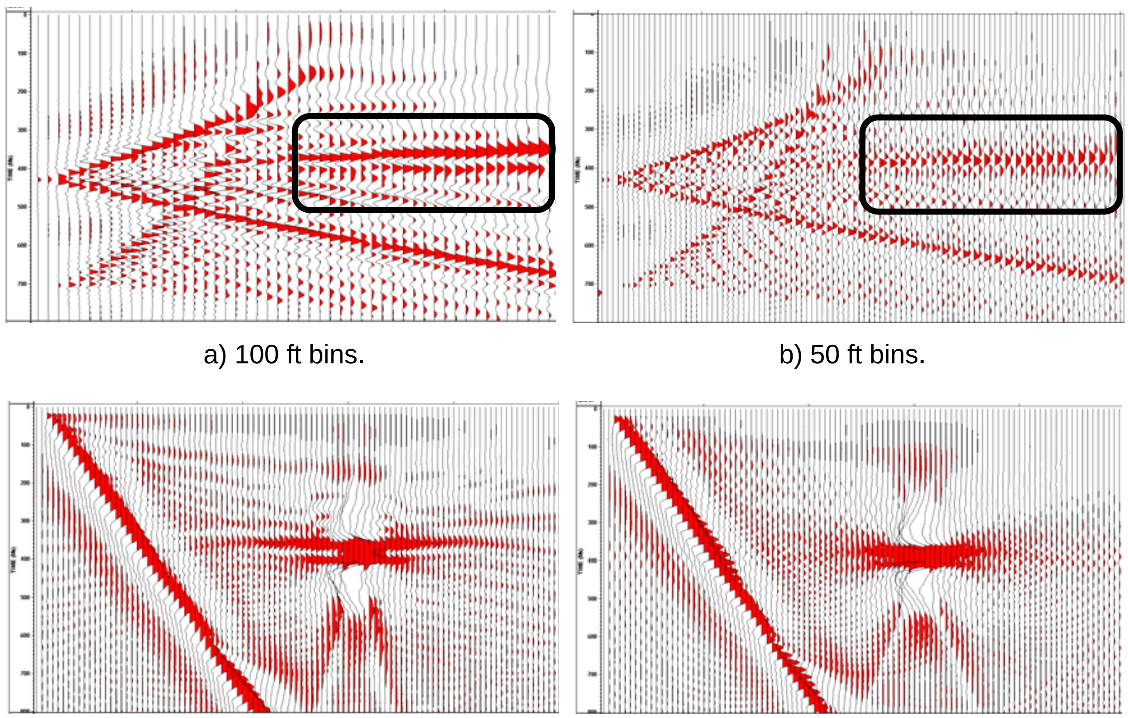

a) 100 ft bins. b) 50 ft bins.

c) d)

FIG. 3. Scattered energy in an EO gather that formed with bin interval the same as the CMP interval, and b) with half the bin interval. `(trace 2601 to 2650, and 2601 to 2700)`

SHALLOW NOISE PROBLEM

When a single input trace is summed into an equivalent offset gather, the equivalent offset may span a number of offset bins. The <u>times</u>, when the equivalent offset (EO) makes a transition from one bin to another, are easily calculated, and a simple implementation of the algorithm would store the data in the corresponding bins. Many traces are summed into each bin with random residual moveout that produces a smoothing effect equivalent to that of an antialiasing filter. Energy is now confined to fixed bin intervals that can lead to imaging artefacts. We will examine this effect from a perspective of one input sample on a given offset trace.

One input sample at a fixed source-receiver offset *h* will be summed into all neighbouring gathers at the same time. Consider Equation (3) simplified into the following hyperbolic form

$$h_e^2\left(x\right)=x^2\left(1-\frac{4h^2}{T^2V^2}\right)+h^2\,. \tag{5}$$

The energy from a single input offset sample is mapped to the neighbouring EO gathers whose location is defined by *x*. This mapping defines the equivalent offset hyperbola shown in Figure 4a. Energy from this spatial hyperbola can then be mapped with moveout directly to the prestack migration ellipse as illustrated in FIG. 4b.

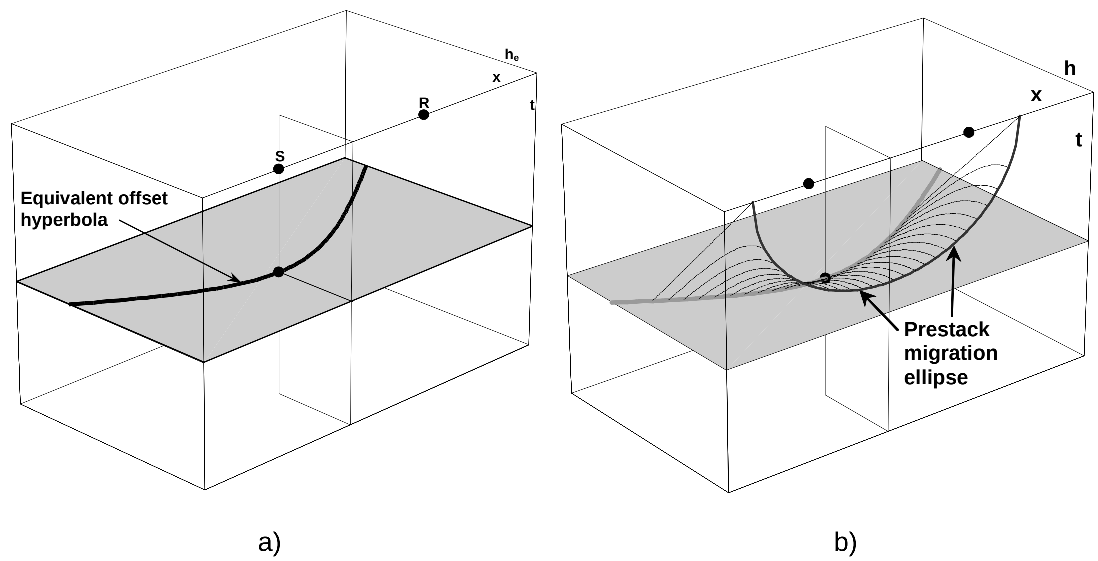

FIG. 4. One input offset sample in the prestack volume is shown in a) being mapped to neighbouring gathers along the equivalent offset hyperbola, and b) moveout correction mapping the energy to the zero offset prestack migration ellipse.

Now consider the case when the offsets have a finite bin interval. The spatial hyperbola will have discrete steps as illustrated in Figure 5a, which will produce discrete steps in the prestack migration ellipse as illustrated in (b). It is these discrete steps that produce migration noise, especially in the shallower parts of a migrated section.

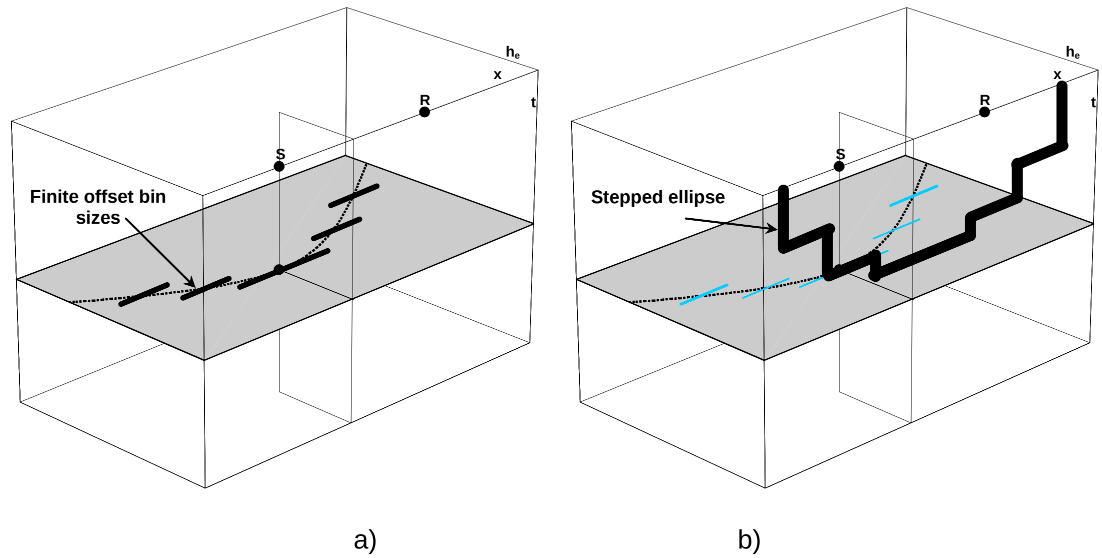

FIG. 5. Equivalent offset hyperbola confined to finite bin sizes.

One method to reduce this discontinuity effect would be to use a very small bin size, but that would then require larger amounts of memory to store the gathers. A simple change to the algorithm would prevent the summing of input energy into a single bin, as illustrated in Figure 6a, but rather distribute the energy to the offset bins on either side of the actual equivalent offset. The amplitudes are weighted proportionally to the relative to the distance to the bin, as schematically illustrated in (b).

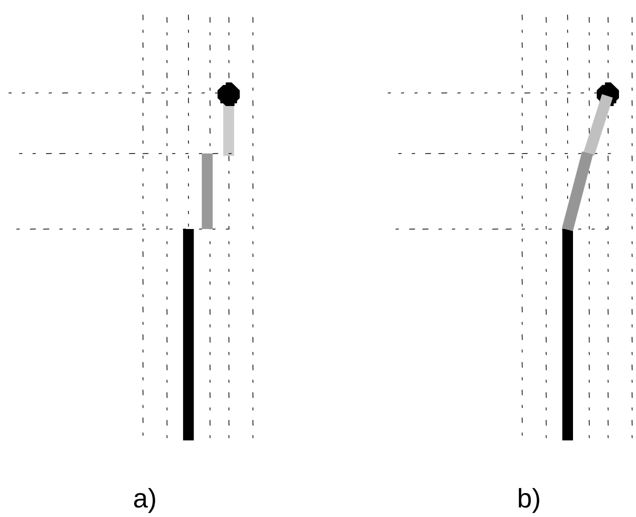

FIG. 6. Illustration of a) input trace-mapped into separate offset bins, and b) the amplitudes of the input trace are linearly distributed between offset bins.

The effect of including this bin interpolation is illustrated in Figure 7. Part (a) shows an ideal prestack migration of two offset points (really wavelets) that produce two smooth prestack migration ellipses. The result of using a large EO bin size is shown in (b) where the stepping effects on the ellipse become obvious. This effect is more subtle but still present in (c) that uses an appropriate bin size. The effect of the bin interpolation is shown in (d), and is quite comparable with the ideal in (a).

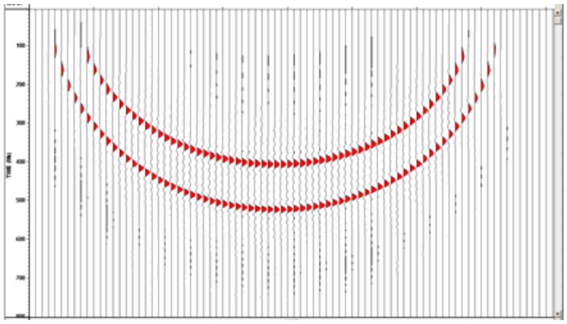

a) Ideal ellipse with 25 ft bin interval.

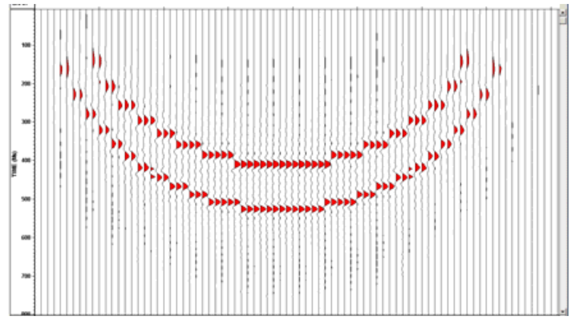

b) Large bin interval of 100 ft.

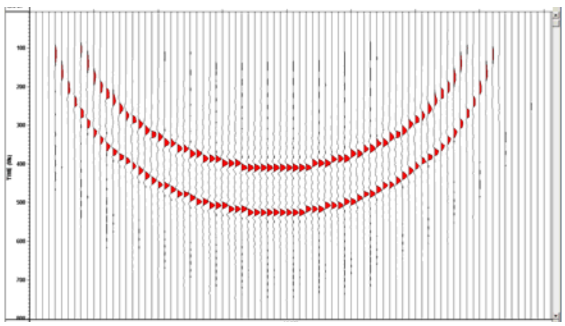

c) 50 ft bins, no EO interpolation.

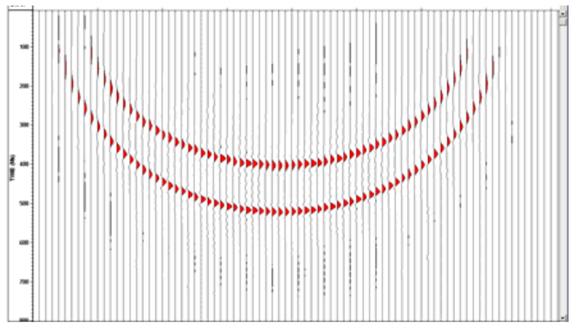

d) 50 ft bins with EO interpolation.

FIG. 7. Prestack migration ellipse for: a) an ideal prestack migration; b) exaggerated example using large bin interval; c) typical bin interval; and d) a typical bin interval with bin interpolation.

ANTIALIASING FILTERS

The differential moveout across the bins acts as an antialiasing filter (AAF). This is one reason why EO migrations have much less noise than comparable prestack Kirchhoff migrations. Figure 8 compares a conventional prestack Kirchhoff migration with an EO prestack migration that does not use an AAF. Note the reduced noise level in the EO migration. (I assume that the migration in (a) did not use an AAF).

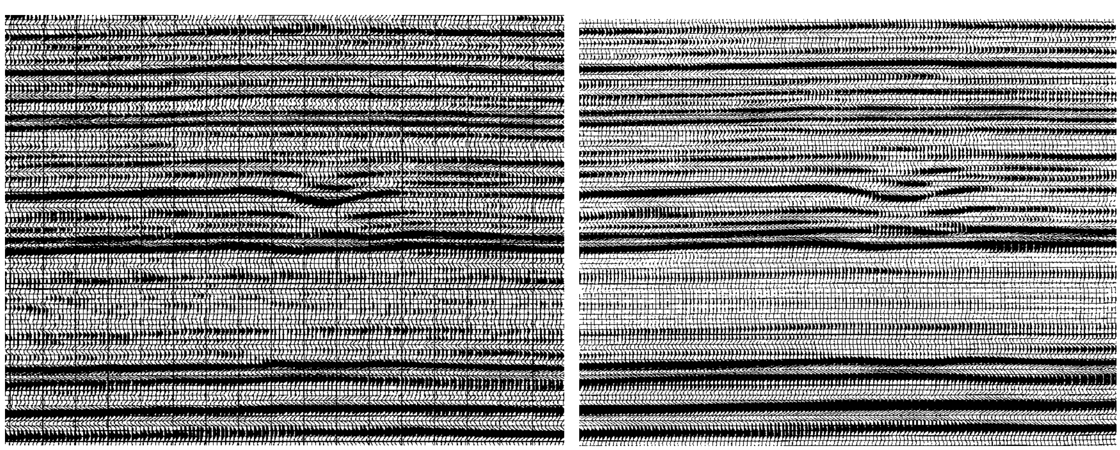

FIG. 8. Prestack migration using: a) a conventional prestack Kirchhoff migration; b) an EO prestack migration.

The boxcar size of this "natural" filter is approximately half the size of one designed by the aliasing equation (4). Consequently, the inclusion of an additional AAF can further reduce noise if desired. Normally this additional noise removal is not required, especially when comparing the images in Figure 8, but may have value when performing deconvolution after migration. Figure 9 is an EO migration of the model that now includes the additional AAF, and should be compared with those in Figure 3.

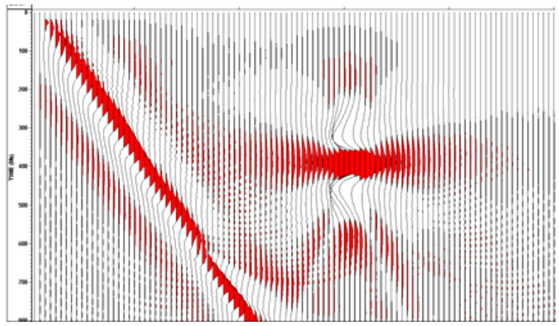

FIG. 9. Addition of an AAF to reduce background aliasing noise. Compare this result with the images in Figure 3.

CONCLUSIONS

Three methods for improving the quality of an EO migration were discussed. The first approach was to choose a bin size for the EO gather that is smaller than either one defined by the aliasing equation, or one defined by half the CMP interval. A second method for improvement advocated summing the input trace into two bins, with weightings proportional to the distance from each bin. The final method suggested the possible use of additional antialiasing filters.

REFERENCES

Bancroft, J. C., Geiger, H. D., and Margrave, G. F., 1998, The equivalent offset method of prestack time migration: Geophysics; **63**, 2042–2053.